Geophysical Research Letters

RESEARCH LETTER
10.1029/2018GL079928

First In Situ Seismic Record of Spreading Events at the Ultraslow Spreading Southwest Indian Ridge

M. Meier[1,2] **and V. Schlindwein**[1]

[1] Geosciences/Geophysics Division, Alfred Wegener Institute, Helmholtz Centre for Polar and Marine Research, Bremerhaven, Germany, [2] Department of Geosciences, University of Bremen, Bremen, Germany

Key Points:
- First seismic in situ record of a spreading event at an ultraslow spreading mid-ocean ridge
- Two migrating earthquake swarms indicate downward intrusion of dikes
- Long-lasting tidally modulated harmonic seismic tremor potentially caused by enhanced hydrothermal circulation after dike intrusion

Supporting Information:
- Supporting Information S1
- Table S1

Correspondence to:
M. Meier,
michaela.meier@awi.de

Citation:
Meier, M., & Schlindwein, V. (2018). First in situ seismic record of spreading events at the ultraslow spreading Southwest Indian Ridge, *Geophysical Research Letters*, *45*, 10,360–10,368. https://doi.org/10.1029/2018GL079928

Received 5 SEP 2018
Accepted 24 SEP 2018
Accepted article online 1 OCT 2018
Published online 10 OCT 2018

Abstract In situ observations of mid-ocean ridge spreading events are rare, and no observations exist at ultraslow spreading ridges. In 2013, two earthquake swarms and prominent, tidally modulated harmonic tremor were accidentally recorded by ocean bottom seismometers at the Southwest Indian Ridge. After relative relocation, the first swarm shows downward migrating hypocenters, while the second swarm immediately spreads over a steeply dipping plane originating at the same location as the first swarm. The tremor signal is temporally connected to the swarms and persists for more than 20 days after the second swarm. Polarization analysis points to two source locations above the seismically active area at 2- to 8-km depth. We interpret swarms and tremor as evidence for a dike intrusion event that caused disruption to an existent hydrothermal system. The tremor may be generated by enhanced hydrothermal circulation caused by the added heat of the intrusion with increased flow during low tides.

Plain Language Summary At mid-ocean spreading ridges, tectonic plates drift apart and magma constantly fills the gap between the plates producing fresh seafloor. At the slowest spreading ridges, very little melt is produced and volcanism happens rarely at widely spaced volcanic centers. Seafloor observations of submarine eruptions from these ultraslow spreading ridges do not exist. We instrumented a seismically active volcano on the ultraslow spreading Southwest Indian Ridge with ocean bottom seismometers. The records revealed two small earthquake swarms along with long-lasting harmonic tremor signals that were strongly influenced by the Earth's tides. We located the source of earthquake swarms and tremor and analyzed their temporal relation. We interpret the migrating earthquake swarms to be caused by moving magma at a depth of about 6 km below the seafloor, heating the area. At the same time water circulates through cracks in the rocks above. The earthquakes may change the water flow paths and the flow is intensified by the heating. This produces the tremor that increases at low tides when the confining water pressure is smaller. Our accidental record of a magmatic spreading event at closest distance shows, for the first time, how magma intrusions drive deep water circulation at ultraslow spreading ridges.

1. Introduction

At spreading ridges new oceanic lithosphere is built by magmatic and tectonic processes, but in situ observations of magmatic eruptions are still very rare. In 1993 Dziak et al. (1995) hydroacoustically monitored dike intrusions at the Juan de Fuca Ridge. The epicenters of the earthquake swarm migrated, and at the terminus of migration a hot water plume and fresh lava flows on the seafloor were detected afterward confirming the assumption of migrating magma. Later, eruptions were also observed by ocean bottom seismometers (OBSs), for example, by Tolstoy et al. (2006) at the fast spreading East Pacific Rise. At the slow spreading Mid-Atlantic Ridge Dziak et al. (2004) observed earthquake swarms and found evidence for dike intrusions.

At ultraslow spreading ridges (<20-mm/year full spreading rate), volcanism is not present continuously along the ridge axis but is focused in specific regions and occurs rarely. In situ observations of volcanic activity do not exist. Nevertheless, indirect evidence for volcanic activity has been found, for example, strong seismicity (Müller & Jokat, 2000; Schlindwein, 2012; Tolstoy et al., 2001), hydrothermal event plumes (Edmonds et al., 2003), and many hydrothermal plumes (Baker et al., 2004; German et al., 1998).

The ultraslow spreading Southwest Indian Ridge between Africa and Antarctica (see Figure 1) shows anomalously low crustal thickness of around 3 km and deep axial rift valleys at its easternmost part. The reduced magmatism in this region is interrupted by prominent volcanic centers at Segments 8, 11, and 14

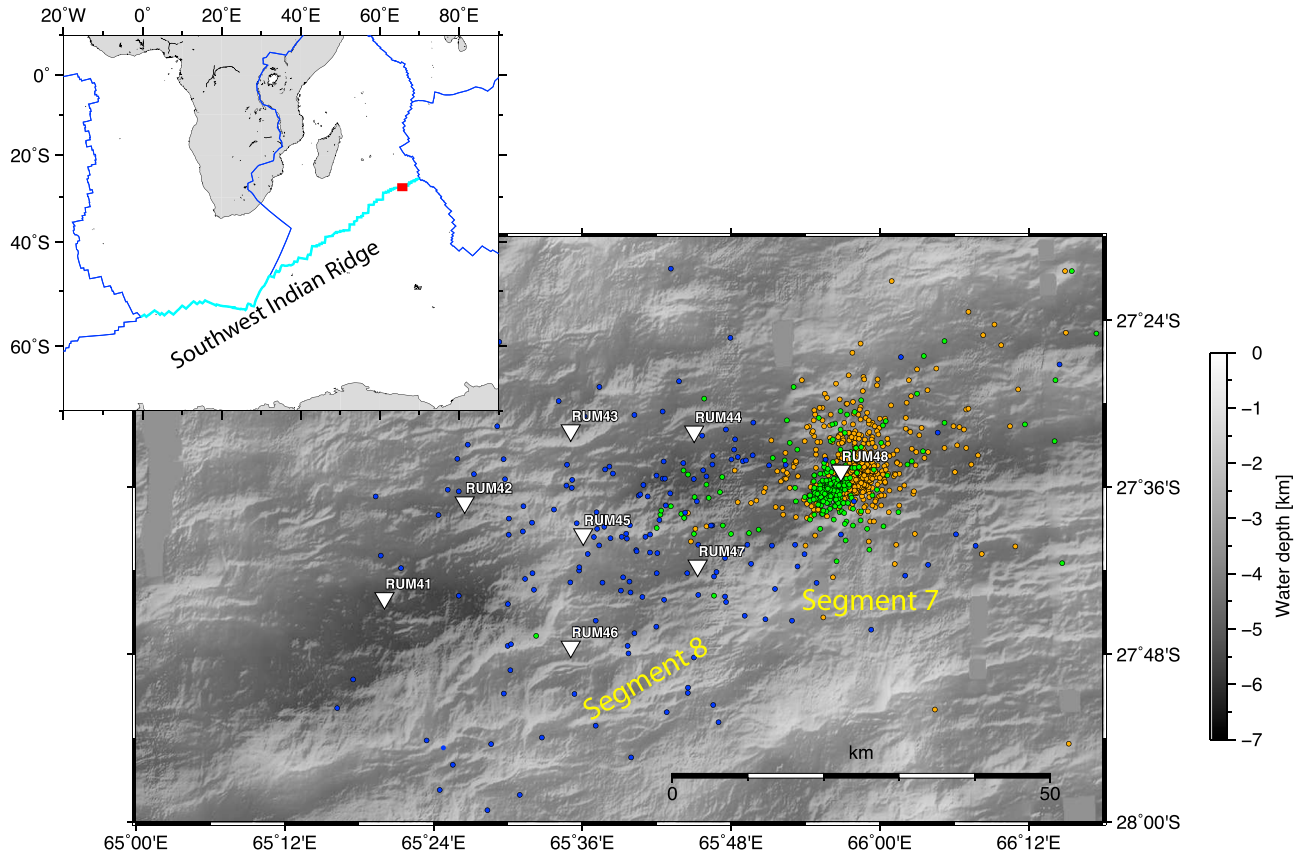

Figure 1. Overview map. Blue lines: plate boundaries according to Bird (2003); light blue: Southwest Indian Ridge. The study area is indicated by the red square. Study area map: teleseismic earthquake swarms (blue) and absolutely located microearthquake swarms in January (orange) and April (green). Triangles mark ocean bottom seismometer positions with their names. The elevation at station RUM45 is the Segment 8 volcano. Bathymetry from Cannat et al. (2006).

(Cannat et al., 2003) with locally thicker crust. These major volcanic centers may be connected to magmatic segments with less pronounced relief as the Segment 7 (Sauter et al., 2001). Repeated teleseismically recorded earthquake swarms between July 1996 and November 2001 (Schlindwein, 2012) led us to instrument the Segment 8 volcano with eight OBS recording from October 2012 to June 2013 (for survey details see Schmid et al., 2017). Schmid et al. (2017) found from local earthquake tomography a low-velocity region near station RUM45 (Figure 1) underneath the volcanic edifice interpreted as a magma chamber. With two local earthquake swarms and harmonic seismic tremor at station RUM48, they found further indications that the instrumented region is currently volcanically active.

In this paper, we analyze in detail these rare and accidental in situ observations of magmatic activity at an ultraslow spreading ridge.

2. Observations and Analysis

2.1. Swarm Activity

We used a correlation trigger with one good signal to noise ratio event per swarm out of a set of tested events to find all earthquakes belonging to the swarms starting on 2 January and 23 April 2013. Since this added only very few locatable events to the existing list of manually identified events, we did not use further template events. All events were reviewed by an analyst, and only events with at least three *P* phase picks and one *S* phase pick were considered for the following location. We used the linear least squares algorithm Hyposat (Schweitzer, 2001) and the one-dimensional velocity model by Schlindwein and Schmid (2016) for preliminary location (Figure 1). All events were relocated with HypoDD (Waldhauser, 2001) to study their spatiotemporal evolution (earthquake catalog in the supporting information).

Relative location was carried out for each swarm individually and together. Besides the catalog data, cross-correlation data were used as input for HypoDD with a correlation coefficient >0.85. We included all

events within a 5-km radius around station RUM48 in the relocation, considering events with less than 0.8-km distance as strongly linked. In the following HypoDD relocation both *P* and *S* phases were considered and the start for the conjugate gradient inversion was the Hyposat location of the events. Several sets of weighting parameters were tested. We chose a parameter set with 45 inversion steps, which showed a robust solution, also achieved by using different parameter sets. Relative location uncertainties range within tens of meters.

The earthquake magnitudes were determined according to Bullen (1985) based on hypocentral distance.

In January 234 events and in April 114 events could be relocated (Figure 2). The magnitudes range between −0.7 and 2.5. The earthquakes in January are located within an area with a diameter of about 10 km east of station RUM48 (Figure 2a). The earthquakes in the west occur at shallower depths of around 5–8 km below seafloor (Figure 2b). In the east depths of 7–13 km below seafloor are observed. Hypocenters deepen from west to east by approximately 5 km. Furthermore, we observed a hypocenter migration within the first 6 hr of this earthquake swarm (2 January 2013 07:00–13:00). This migration runs to the northeast and downward with a velocity of 0.43 ± 0.1 m/s (Figure 2e) at an angle of about 45° from the horizontal.

The April events are scattered over a smaller area (of around 6 km) than the January events (Figure 2c). The events dip at an angle of 60° from about 5 km in the west to a maximum of 14 km in the east, but a migration is not observed. For both swarms, higher-magnitude events tend to occur in deeper areas. A tidal modulation of earthquake occurrence or indications of eruptive activity were not observed.

2.2. Seismic Tremor

Prominent seismic tremor was observed at station RUM48 in connection with the earthquake swarm activity (Figure 3). Tremor was not observed on the neighboring seismic stations. It appeared clearly on the seismometer records but is less visible on the hydrophone channel. The fundamental frequency of the tremor in December/January varies between 0.5 and 1.25 Hz. Clearly spaced narrow harmonic frequency peaks appear at around 1.75, 4.5, and 6.5 Hz (Figure S1). The tremor occurs in bursts of several hours visible both in the spectrogram (Figure 3a) and in the waveforms (Figures S1 and S2). The tremor episode in April is more continuous and of higher amplitude. The fundamental tremor frequency increases during the first days and varies between 1.25 and 1.75 Hz before it returns to lower frequencies of 0.5–1.5 Hz. Harmonics are also clearly present, but the spectra are more complicated (Figure S1). While the fundamental frequency and its amplitude rhythmically vary with phases of low-frequency tremor having low amplitude, the spectral band at about 4.5 Hz appears to be present over time, varying only in spectral amplitude. The tremor again occurs in bursts with two strong tremor episodes per day.

To analyze the tremor periodicity, we extracted the maximum spectral amplitude and the corresponding frequency in the frequency band of the fundamental frequency between 0.49 and 1.4 Hz (January) and 0.49 and 2.0 Hz (April). The resulting frequency-time (Figure 3, black line) and amplitude-time curves were low-pass filtered with a running average filter of about 45-min length and subjected to a frequency analysis to resolve tidal constituents (Figure S3; tidal signal according to Egbert & Erofeeva, 2002). Both tremor amplitude and fundamental frequency show a 12-hr periodicity.

To examine the time relation between seismic swarms and tremor in more detail, we searched for tremor signals during the entire recording period. Based on the method of McNamara and Buland (2004), we estimated the average spectral power in the frequency band between 0.7 and 4 Hz containing the fundamental tremor frequency. Figure 4 shows hourly values shifted by 30 min (black line) and daily averages (red). We declared tremor when these daily averages exceeded −122 db. A waveform analysis of the tremor signals further showed that the particle motion of the tremor signals is almost linear (Figure S2), suggesting body waves. We therefore independently used the polarization characteristics to search for tremor. A polarization analysis after Flinn (1965) was performed for consecutive 10-min windows of the signal filtered between 0.7 and 4 Hz. We chose the fundamental frequency of the tremor for polarization analysis as it contains the longest wavelength signals that are less likely to be distorted by subsurface heterogeneities. Figure 4 shows 1-hr running means of rectilinearity and planarity of the tremor signal. We declared seismic tremor when a hourly average rectilinearity of 0.6 was exceeded. Both tremor definitions highlighted the main tremor phases preceding and following the January swarm and a long-lasting episode starting shortly before the April swarm and lasting for more than 28 days. An additional short tremor phase was recognized around 8 March 2013 and is also connected to a minor increase in seismicity rate not detected before.

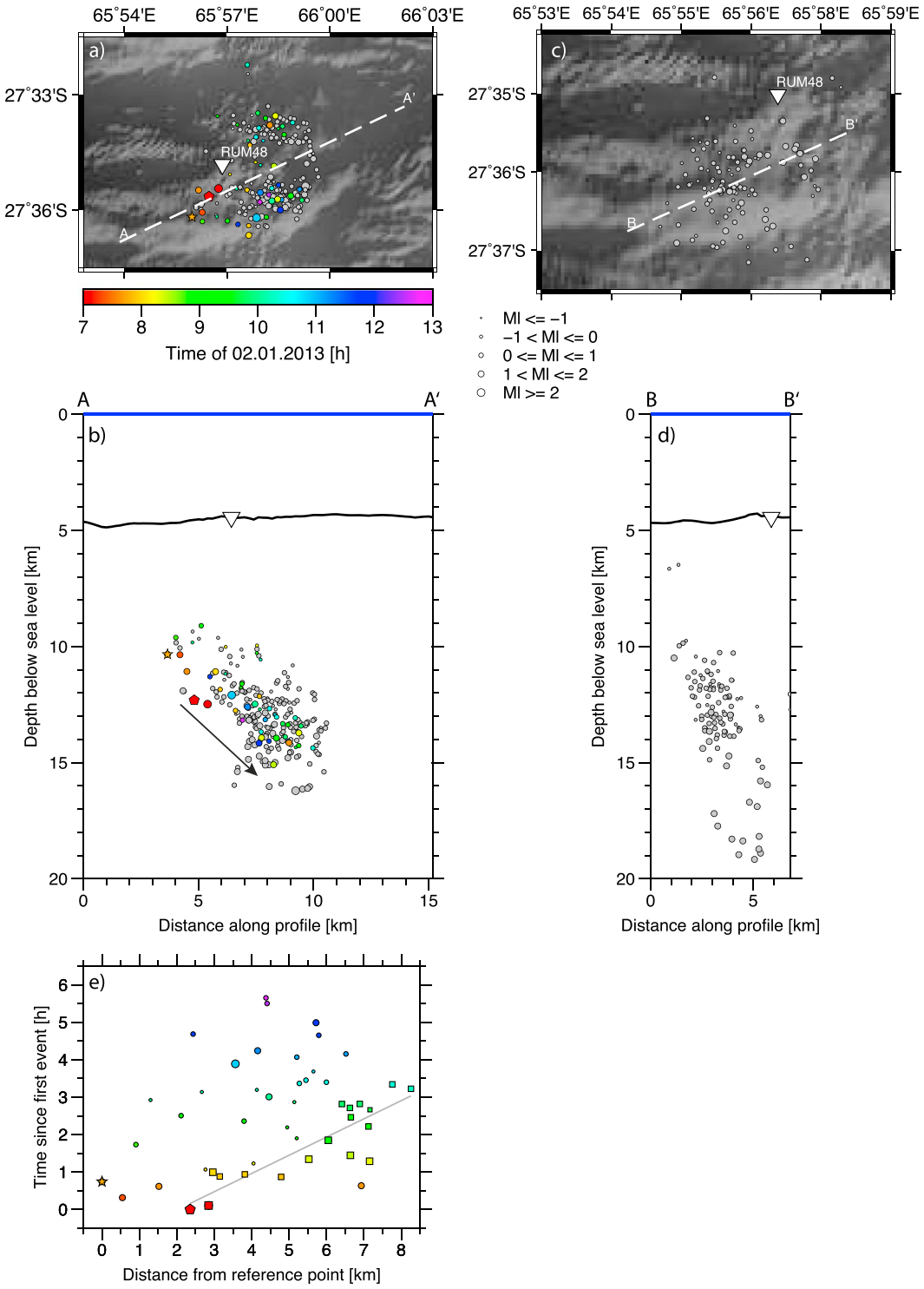

Figure 2. (a) Relative relocation results for swarm in January. Colors indicate origin time of events during the first 6 hr of the swarm; gray: remaining hypocenters. Circles scale with magnitude M_l. (b) Cross section along dashed line in (a) with hypocenters projected onto profile. Arrow indicates direction of migration. (c) Relocation of April swarm; no migration was observed here. (d) Projection of April hypocenters onto profile in (c). (e) Time since first event (pentagon,M_l = 0.6) over distance from reference point (star, M_l = 1.2). Squares mark events used for migration velocity calculation (linear regression shown as gray line). The early event at a distance of approximately 7 km was excluded, assuming it occurred as background seismicity.

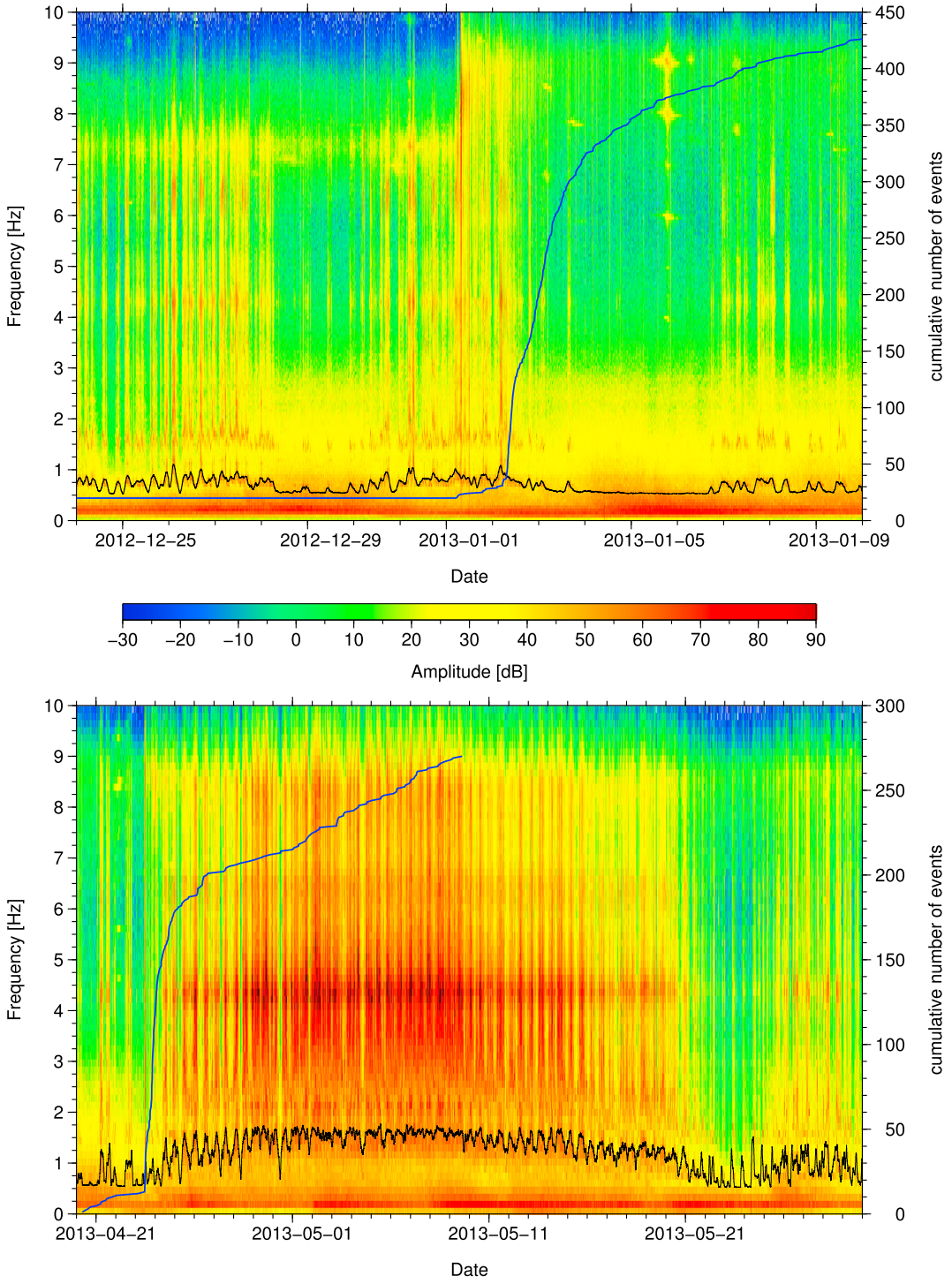

Figure 3. Spectrogram of tremor signal in January (upper) and April (lower). Blue line: cumulative number of all Hyposat located events within the area 65°51′E to 66°03′E and 27°30′S to 27°42′S. Black line: maximum spectral amplitude and corresponding frequency within the fundamental frequency band 0.49–1.4 Hz (January) and 0.49–2.0 Hz (April).

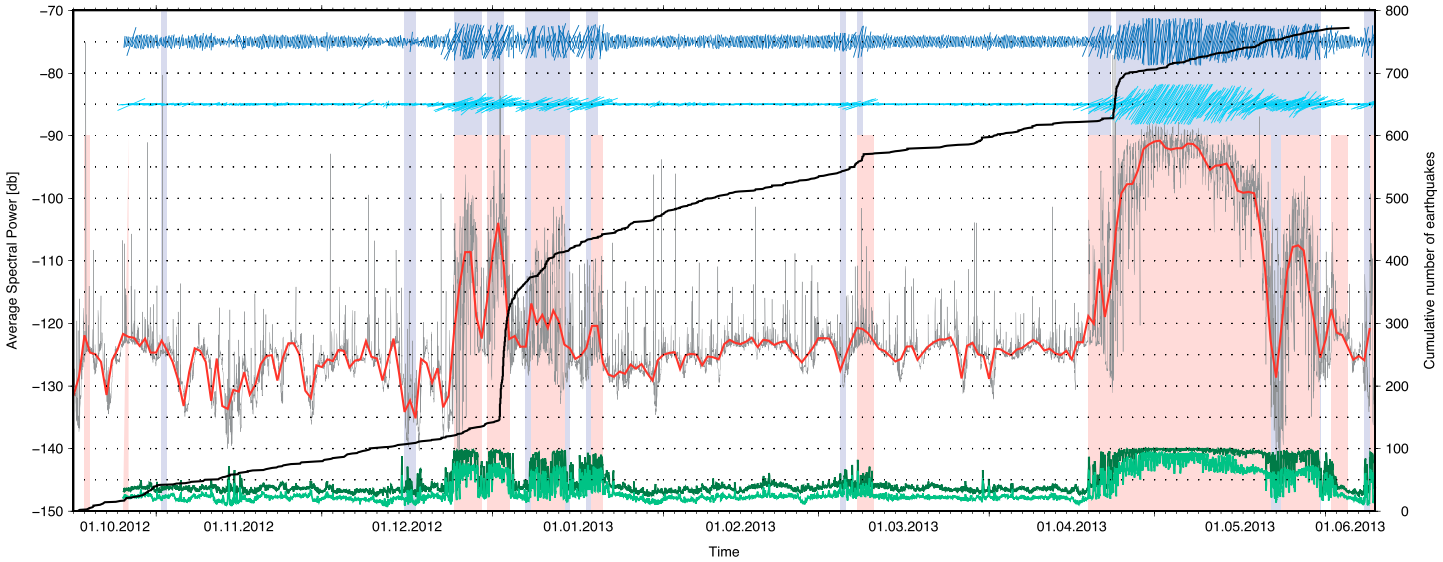

Figure 4. Occurrence and characteristics of seismic tremor over the recording period. Solid black line indicates cumulative seismicity curve with events within 65°51′E to 66°03′E and 27°30′S to 27°42′S. From top to bottom: Dark blue: azimuth of tremor, north represents vertical and light blue: incidence angle of tremor with respect to vertical. For clarity only 1 value per 10 hr is plotted. Line length indicates rectilinearity, filter 0.7–4 Hz. Gray: Hourly average spectral power between 0.7 and 4 Hz overlapping by 50%, and red: daily average. Dark green: hourly values for planarity and light green: rectilinearity of tremor signal filtered 0.7–4 Hz. Tremor is declared if rectilinearity exceeded 0.6 (blue boxes) or if daily spectral power exceeded −122 db (red boxes).

The polarization analysis further yielded back azimuth and incidence angle of the tremor signal. Figure 5 illustrates these different directions for tremor before and after 1 April counting only polarized 10-min-long signals with a rectilinearity > 0.75 in bins of 5°. The tremor in January, March, and April prior to the onset of the seismic swarm points to a shallow source in a south-southwesterly direction (Figure 5a). With the onset of the April seismic swarm, the tremor particle motion points to a more southerly and deeper source (Figure 5b).

3. Interpretation

The presence of a magma chamber underneath the nearby Segment 8 volcano, which was probably installed during the teleseismic swarm period 1996–2002 (Schlindwein, 2012; Schmid et al., 2017) may indicate that the observed earthquake swarms occurred in the context of a long-lasting spreading event.

Earthquake swarms with migrating hypocenters and accompanying tremor signals are commonly interpreted as resulting from magma (Bohnenstiehl et al., 2008). Our observation of migrating hypocenters during the first hours of the January swarm and tremor signals accompanying both swarm periods is therefore indicative for a magmatic intrusion. Interestingly, the migration has a downward direction with a significant angle with respect to the horizontal. Migration starts at the same depth as the magma chamber underneath the Segment 8 volcano. Comparable low-velocity anomalies or *S* phase delays as on station RUM45 are missing. However, since the swarms were recorded accidentally, the network geometry was not optimized to resolve a melt region beneath station RUM48. Both swarms in January and April show a common initiation point close to station RUM48. The smaller March swarm is located northeast of the other swarms and might rather represent a further extension of the January swarm (Figure 5c). The migration velocity in January is similar to earlier observed migration velocities (e.g., Belachew et al., 2011). According to Rubin and Gillard (1998) only events with maximum magnitudes of 1 are caused by a propagating dike tip itself. Earthquakes with higher magnitudes reflect ambient stresses in rocks near to failure and not the dike itself. The earthquakes used to calculate the propagation velocity show magnitudes up to 2.1. Therefore, the determined velocities might not represent the dike tip propagation, but rather the stress release as the intrusion plane opens. We thus assume that both earthquake swarms directly image dike migration or indirectly monitor stress release around an intrusion plane. Both intrusions are potentially fed from a common reservoir near their starting point.

Seismic tremor is related in time and space to the intrusions. The polarization analysis of the seismic tremor consistently points to two tremor sources south-southwest of station RUM48. The distance from the station is unknown, but the lack of the tremor signal at the neighboring stations limits the distance to the tremor source

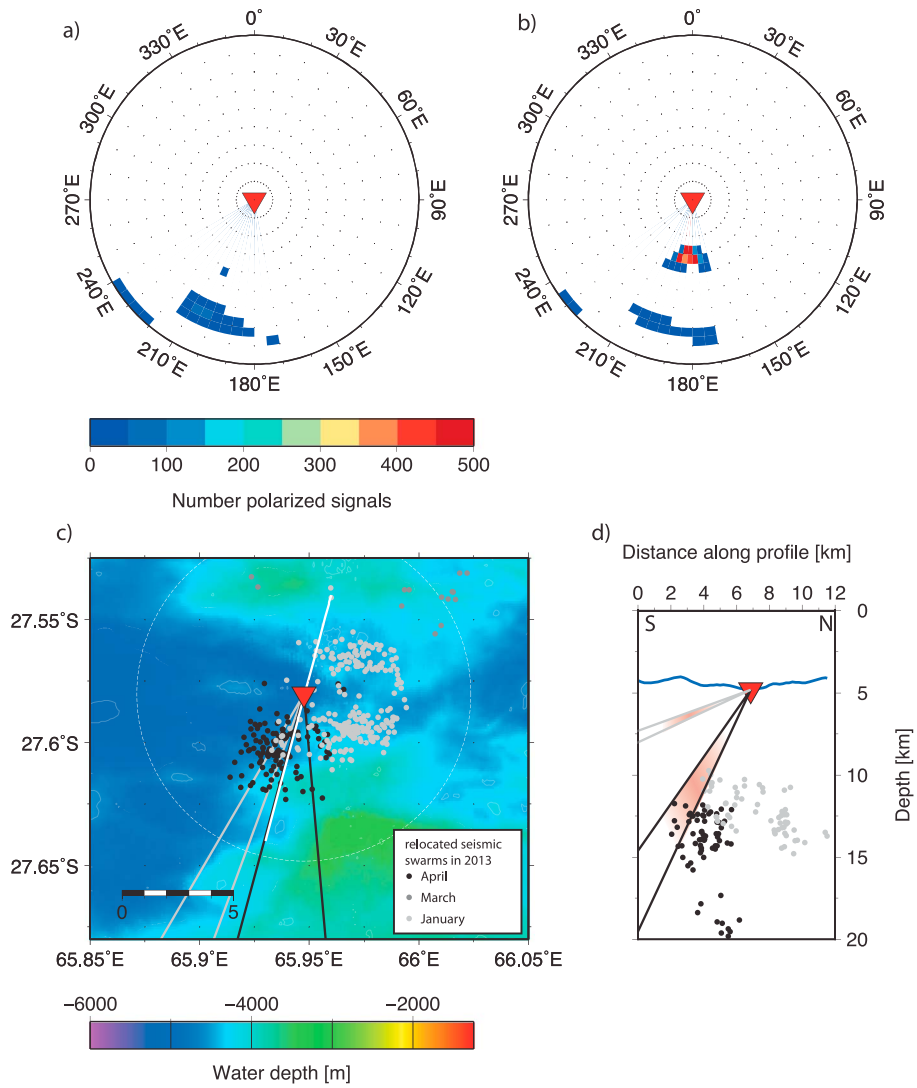

Figure 5. Source of tremor signal. Provenance of well-polarized signals with rectilinearity >0.75 (a) before 1 April and (b) after 1 April. Vertically incident signals plot in the center, horizontally incident signals on the margin of the circle. (c) Map view of relocated swarms and direction of tremor from (a) as gray lines and (b) as black lines. Only direction of most frequent polarized signals is indicated. Dashed circle indicates one third of distance to nearest seismic station from station RUM48 (red triangle) as estimated maximum distance to tremor source. White line: cross section in (d). (d) Cross section through topography (blue line) with earthquakes within 1 km of profile projected. Incidence angle range of tremor is indicated: gray before 1 April and black after 1 April. Shaded areas represent likely tremor source location as discussed in the text.

to an estimated maximum of about 7.5 km, a third of the distance to the next stations (Figure 5c). Monigle et al. (2009) found in their study no correlation between tremor observed at different OBSs located only few kilometers apart, suggesting that the tremor source here may even be closer to the OBS than 7.5 km. We prefer a tremor source area about 2–4 km from station RUM48 that shows seismicity during both swarms and is marked by an east west trending ridge. The cross sections in Figure 5d show that the tremor signal comes clearly from above the seismicity. In January, a shallow source potentially above the area where both intrusions initiated is likely. In April the tremor source is deeper. Again, a source location near the swarm initiation point appears likely. In either case, the tremor is produced at shallower depth than the intrusion seismicity. We therefore conjecture that the tremor is not caused by magma flow within the intrusion plane, but rather by hydrothermal circulation above the dike intrusions. Hydrothermal event plumes accompanying intrusion events have been reported, for example, for the Gakkel Ridge (Edmonds et al., 2003) or the Carlsberg Ridge (Murton et al., 2006). Along ultraslow spreading ridges, unexpectedly high hydrothermal activity has been

observed (Van Dover, 1998). Assuming hydrothermal circulation near a magmatic intrusion therefore appears justified although no event plume was reported from this area, because no measurements were made.

We envisage a scenario, where a hydrothermal system already exists prior to the January swarm. Magma accumulation in a reservoir near the starting point of both intrusions may provide heat to enhance hydrothermal flow and cause tremor episodes already before the onset of the January swarm. The swarm caused a disruption to the hydrothermal system that enhanced flow and led to shallow tremor in January, March, and prior to the April earthquake swarm. In April, seismicity immediately occurred on the entire intrusion plane indicating a rapid opening. Tremor starts almost at the same time with an increase in both tremor amplitude and frequency. Tremor is now excited at greater depths in the hydrothermal system and overprints the shallower source, if it is still active at that time. We consider the long duration of the April tremor—exceeding by far the intrusion seismicity—a further sign that the tremor is not caused by magma flow but by enhanced hydrothermal flow driven by the heat of the intrusion.

Another feature of the tremor signal indicating that the tremor might be caused by hydrothermal circulation is the tidal modulation of the tremor signal seen in the frequency analysis of both tremor frequency and amplitude with higher tremor amplitude during low tides. Tidally modulated tremor has been found at other hydrothermal systems. Monigle et al. (2009) found comparable harmonic tremor at OBS on the East Pacific Rise that was attributed to hydrothermal flow in cracks close to the OBS. There, too, tremor pattern changed in connection with a magmatic event. For hydrothermal systems a tidal modulation of exit temperatures has been postulated to result from changes in flow speed induced by tidal loading (Barreyre et al., 2014). Such changes in flow speed could affect both tremor amplitude and frequency, with higher amplitudes being expected for higher flow rates.

The detailed generation of the seismic tremor signals is generally not fully understood. Several models exist that suggest flow through narrow cracks or past constrictions (e.g., Chouet, 1986) or oscillation in cavities (e.g., Julian, 1994). A detailed tremor source analysis would require additional data constraining for example flow rate or temperature changes in a supposed hydrothermal system.

4. Conclusions

We analyzed seismic records of earthquake swarms and conspicuous tidally modulated tremor accidentally recorded at the ultraslow spreading Southwest Indian Ridge during a potential spreading episode. The observed earthquake swarms in January and April 2013 are assumed to reflect dike intrusions. The swarm seismicity shows a downward migration and might image the stress release around the opening intrusion plane. The observed seismic tremor signal is in time and space related to the earthquake swarms. We suggest a source area close to station RUM48 and above seismicity, which together with the timing of the onset of tremor activity and its tidal modulation serves as evidence that the tremor is produced by hydrothermal circulation. We propose that the circulation is already present before the swarm activity but is altered by the earthquakes and enhanced by the heat of the intrusion. Since this magmatic event was captured accidentally, no further data exist to verify this interpretation. However, our study shows that spreading episodes at ultraslow spreading ridges may last over many years, giving the opportunity to comprehensively instrument active sites.

Acknowledgments
We acknowledge crew and scientists of cruises R/V Marion Dufresne MD192 and R/V Meteor M101 for their support in the OBS operations. Instruments were provided by the DEPAS pool for amphibian seismology and deployed within the framework of the RHUM-RUM project (http://www.rhum-rum.net), which was funded through German Science Foundation (subgrant SCHL 853/3-1 to V. S.), Agence de la Recherche, France (project ANR-11-BS56-0013), and Institute Polaire Paul Emile Victor, France. M. M. was funded through German Science Foundation grant SCHL853/1-1. The RHUM-RUM data set with FDSN network code YV can be obtained from the RESIF data center (http://seismology.resif.fr).

References

Baker, E. T., Edmonds, H. N., Michael, P. J., Bach, W., Dick, H. J. B., Snow, J. E., et al. (2004). Hydrothermal venting in magma deserts: The ultraslow-spreading Gakkel and Southwest Indian Ridges. *Geochemistry, Geophysics, Geosystems*, *5*, Q08002. https://doi.org/10.1029/2004GC000712

Barreyre, T., Escartin, J., Sohn, R. A., Cannat, M., Ballu, V., & Crawford, W. C. (2014). Temporal variability and tidal modulation of hydrothermal exit-fluid temperatures at the Lucky Strike deep-sea vent field, Mid-Atlantic Ridge. *Journal of Geophysical Research: Solid Earth*, *119*, 2543–2566. https://doi.org/10.1002/2013JB010478

Belachew, M., Ebinger, C., Cote, D., Keir, D., Rowland, J. V., Hammond, J. O. S., & Ayele, A. (2011). Comparison of dike intrusions in an incipient seafloor-spreading segment in Afar, Ethiopia: Seismicity perspectives. *Journal of Geophysical Research*, *166*, B06405. https://doi.org/10.1029/2010JB007908

Bird, P. (2003). An updated digital model of plate boundaries. *Geochemistry, Geophysics, Geosystems*, *4*(3), 1027. https://doi.org/10.1029/2001GC000252

Bohnenstiehl, D. R., Waldhauser, F., & Tolstoy, M. (2008). Frequency-magnitude distribution of microearthquakes beneath the 9°50′N region of the East Pacific Rise, October 2003 through April 2004. *Geochemistry, Geophysics, Geosystems*, *9*, Q10T03. https://doi.org/10.1029/2008GC002128

Bullen, K. E. (1985). *An introduction to the theory of seismology*. Cambridge: Cambridge University Press.

Cannat, M., Rommevaux-Jestin, C., & Fujimoto, H. (2003). Melt supply variations to a magma-poor ultra-slow spreading ridge (Southwest Indian Ridge 61° to 69° E). *Geochemistry, Geophysics, Geosystems*, *4*(8), 9104. https://doi.org/10.1029/2002GC000480

Cannat, M., Sauter, D., Mendel, V., Ruellan, E., Okino, K., Escartin, J., et al. (2006). Modes of seafloor generation at a melt-poor ultraslow-spreading ridge. *Geology*, *34*(7), 605–608. https://doi.org/10.1130/G22486.1

Chouet, B. A. (1986). Dynamics of a fluid-driven crack in three dimensions by the finite difference method. *Journal of Geophysical Research*, *91*, 13,967–13,992. https://doi.org/10.1029/JB091iB14p13967

Dziak, R. P., Fox, C. G., & Schreiner, A. E. (1995). The June–July 1993 seismo-acoustic event at CoAxial segment, Juan de Fuca Ridge: Evidence for a lateral dike injection. *Geophysical Research Letters*, *22*, 135–138. https://doi.org/10.1029/94GL01857

Dziak, R. P., Smith, D. K., Bohnenstiehl, D. R., Fox, C. G., Desbruyeres, D., Matsumoto, H., et al. (2004). Evidence of a recent magma dike intrusion at the slow spreading Lucky Strike segment, Mid-Atlantic Ridge. *Journal of Geophysical Research*, *109*, B12102. https://doi.org/10.1029/2004JB003141

Edmonds, H. N., Michael, P. J., Baker, E. T., Connelly, D. P., Snow, J. E., Langmuir, C. H., et al. (2003). Discovery of abundant hydrothermal venting on the ultraslow-spreading Gakkel ridge in the Arctic Ocean. *Nature*, *421*, 252–256. https://doi.org/10.1038/nature01351

Egbert, G. D., & Erofeeva, S. Y. (2002). Efficient inverse modeling of barotropic ocean tides. *Journal of Atmospheric and Oceanic Technology*, *19*(2), 183–204. https://doi.org/10.1175/1520-0426(2002)019<0183:EIMOBO>2.0.CO;2

Flinn, E. (1965). Signal analysis using rectilinearity and direction of particle motion. *Proceedings of the IEEE*, *53*(12), 1874–1876. https://doi.org/10.1109/PROC.1965.4462

German, C. R., Baker, E. T., Mevel, C., & Tamaki, K. (1998). Hydrothermal activity along the South West Indian Ridge. *Nature*, *395*, 490–493. https://doi.org/10.1038/26730

Julian, B. R. (1994). Volcanic tremor: Nonlinear excitation by fluid flow. *Journal of Geophysical Research*, *99*, 11,859–11,877. https://doi.org/10.1029/93JB03129

McNamara, D. E., & Buland, R. P. (2004). Ambient noise levels in the continental United States. *Bulletin of the Seismological Society of America*, *94*(4), 1517. https://doi.org/10.1785/012003001

Monigle, P. W., Bohnenstiehl, D. R., Tolstoy, M., & Waldhauser, F. (2009). Seismic tremor at the 9°50′N East Pacific Rise eruption site. *Geochemistry, Geophysics, Geosystems*, *10*, Q11T08. https://doi.org/10.1029/2009GC002561

Müller, C., & Jokat, W. (2000). Seismic evidence for volcanic activity discovered in central Arctic. *Eos, Transactions American Geophysical Union*, *81*(24), 265–269. https://doi.org/10.1029/00EO00186

Murton, B. J., Baker, E. T., Sands, C. M., & German, C. R. (2006). Detection of an unusually large hydrothermal event plume above the slow-spreading Carlsberg Ridge: NW Indian Ocean. *Geophysical Research Letters*, *33*, L10608. https://doi.org/10.1029/2006GL026048

Rubin, A. M., & Gillard, D. (1998). Dike-induced earthquakes: Theoretical considerations. *Journal of Geophysical Research*, *103*, 10,017–10,030. https://doi.org/10.1029/97JB03514

Sauter, D., Patriat, P., Rommevaux-Jestin, C., Cannat, M., & Briais, A. (2001). The Southwest Indian Ridge between 49° 15′E and 57° E: Focused accretion and magma redistribution. *Earth and Planetary Science Letters*, *192*, 303–317. https://doi.org/10.1016/S0012-821X(01)00455-1

Schlindwein, V. (2012). Teleseismic earthquake swarms at ultraslow spreading ridges: Indicator for dyke instrusions? *Geophysical Journal International*, *190*, 442–456. https://doi.org/10.1111/j.1365-246X.2012.05502.x

Schlindwein, V., & Schmid, F. (2016). Mid-ocean-ridge seismicity reveals extreme types of ocean lithosphere. *Nature*, *535*, 276–279. https://doi.org/10.1038/nature18277

Schmid, F., Schlindwein, V., Koulakov, I., Plötz, A., & Scholz, J. R. (2017). Magma plumbing system and seismicity of an active mid-ocean ridge volcano. *Scientific Reports*, *7*, 42949. https://doi.org/10.1038/srep42949

Schweitzer, J. (2001). HYPOSAT—An enhanced routine to locate seismic events. *Pure and Applied Geophysics*, *158*(1), 277–289. https://doi.org/10.1007/PL00001160

Tolstoy, M., Bohnenstiehl, D. R., Edwards, M. H., & Kurras, G. J. (2001). Seismic character of volcanic activity at the ultraslow-spreading Gakkel Ridge. *Geology*, *29*(12), 1139–1142. https://doi.org/10.1130/0091-7613(2001)029<1139:SCOVAA>2.0.CO;2

Tolstoy, M., Cowen, J. P., Baker, E. T., Fornari, D. J., Rubin, K. H., Shank, T. M., et al. (2006). A sea-floor spreading event captured by seismometers. *Science*, *314*, 1920–1922. https://doi.org/10.1126/science.1133950

Van Dover, C. L. (1998). Vents at higher frequency. *Nature*, *395*, 437–439. https://doi.org/10.1038/26617

Waldhauser, F. (2001). HypoDD—A program to compute double-difference hypocenter locations U.S: U.S. Geologic Survey Open-File Report 01-113.